SQMS Summer Internship Report
SRF cavities and Superconducting qubits for Gravitational Waves and Dark Photons detection

Roberto Menta[1,5], Anna Grassellino[2,4], Roni Harnik[2,3], and Asher Berlin[3,2]

[1]*University of Pisa, Department of Physics "E. Fermi"*
[2]*Superconducting Quantum Materials and Systems Center, Fermi National Accelerator Laboratory*
[3]*Theory Division, Fermi National Accelerator Laboratory*
[4]*Applied Physics and Superconducting Technology Division, Fermi National Accelerator Laboratory*
[5]*Northwestern University, Department of Physics and Astronomy, Center for Applied Physics and Superconducting Technology*

October 2022

Abstract

The report is a short review which focuses on the employment of a Superconducting Radio Frequency (SRF) cavity for detection of Gravitational Waves (GWs). This first part is inspired by the works of Berlin's group. In the second part, we analyze also the idea to use a cavity-qubit system for the GWs detection and the Dark Photons (DPs) detection. In this case, the starting point is the work of Dixit's group which will be extended for SQMS cavities.

Contents

1 Introduction

Microwave or radio frequency (RF) cavities with superconducting walls are very important for particle accelerators. Indeed, when they are excited at their resonant frequency, they build up large amplitude electromagnetic (EM) field which dissipates very little heat. This makes it possible to provide an extremely conversion of radio-frequency power into energy gain for the charged particle beams that pass through them. Despite of that main application, the SRF cavities are high quality EM resonators which can be employ as sensors for detection of *new physics*. In particular, we are studying them as detectors of non-newtonian gravitational fields and also for Dark Matter candidates like the dark photons.

- In 1971, Braginsky and Menskii [1] suggested using microwave cavities to detect high-frequency gravitational wave (GW).
- In 1978, Pegoraro et al. [2] developed cavities able to operate at much lower (radio) frequencies.

Both high- and low-frequency microwave cavity detectors operate in essentially the same way : a gravitational wave incident on the cavity couples its EM modes and thereby induces transition between modes. The coupling is due to the *direct* interaction between the EM field and the GW and to the *indirect* interaction in which the GW interacts directly with the cavity walls, whose resulting motion couples the EM modes. In 2005, Pegoraro et al. proposed an experiment, so called MAGO [5] which goes this way, i.e. using empty cavity with a EM field inside to detect GW. In this report we would analyze the possibility to develop an experiment which uses a cavity-qubit system. So, the purpose of this report is to understand if there are some advantages using this system for detecting *new physics* respect to MAGO or not. Moreover, we are reporting all ideas and calculations about GW that we thought on the road in this 9 weeks of research. We also are gonna

to talk preliminary about qubit-GW interaction. Finally we are seeing that the dark photon (DM candidate) search will be easier compared with GW one. Moreover, we are revisiting the paper of Dixit et al. [6] to extend the idea of dark photon search with cavity-qubit system to SQMS cavities in different regime of dark photon's mass. We will see that the proposal to use the system in a Fock state with a such huge n (number of photons) is not advantageous respect to Dixit et al.'s protocol.

2 SRF cavity

The SRF cavities are extremely high quality electromagnetic resonators. For quantum computing, quantum states can be stored and manipulated in EM resonators, and superconductors at $T \sim$ mK are able to sustain the coherence of the quantum states for long enough to perform complex computations. For *quantum sensing*, SRF cavities can furnish a large volume where very weak signals of radio-frequency photons can be collocated, with only a small fraction of photons being lost to heat at the cavity walls. Basically, from a theoretical point of view, a Superconducting Radio Frequency (SRF) cavity is an Harmonic Oscillator (HO). We can imagine the cavity like a box with an electromagnetic field inside of that.

1 dimensional model So, let's focus on the HO equation of motion in one dimension ($\hat{x}$, for example) in presence of a *loss* term :

$$\ddot{x}(t) + \omega_0^2 x(t) = A\cos(\omega_{drv} t) - \frac{\omega_0}{Q}\dot{x}(t) \tag{1}$$

where ω_0 is the characteristic angular frequency of the oscillator (here the cavity thought like the detector), ω_{drv} is the frequency of the *driving* term such as the signal of GW. The last term in equation (1) is the loss term that we can think like the dissipation of the signal because of the cavity. For the SRF cavities we have :

- $Q \sim \mathcal{O}(10^{10} \div 10^{12})$ for the superconducting proprieties of the cavities. (SRF)
- $\omega_0 \sim$ GHz (SRF).

Hence, the damping time is $t_{damp} \sim \frac{10^{10\div 12}}{\text{GHz}} \gg$ sec and it is an advantage in the detection. For instance, we report below some numerical simulation of the solution of Equation 1 made by `Mathematica`. In the resonant case, $\omega_{drv} \sim \omega_0$, we have the following two results.

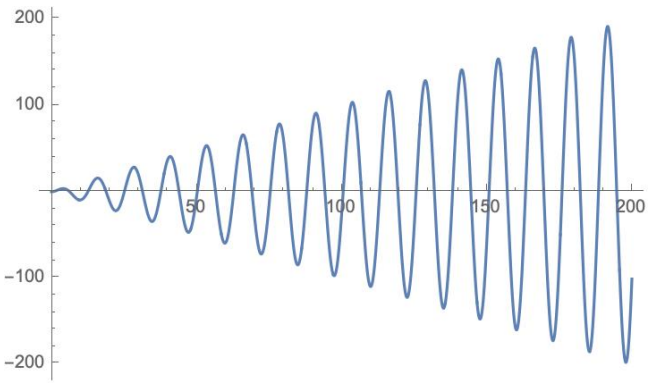

Figure 1: Solution $x(t)$ of equation 1 in absence of the loss term. The trend of the peaks grows linearly in time. The initial conditions fixed are : $x(0) = 0, \dot{x}(0) = 0$. Set parameters : $\omega_0 = \omega_{drv} = 0.5, A = 1$.

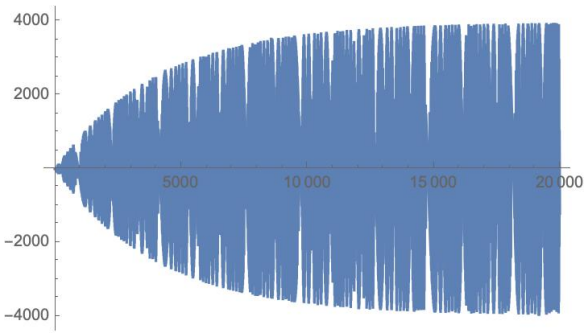

(a) In presence of losses. The initial conditions: $x(0) = 0, \dot{x}(0) = 0$. Set parameters : $\omega_0 = \omega_{drv} = 0.5, A = 1, Q = 10^3$.

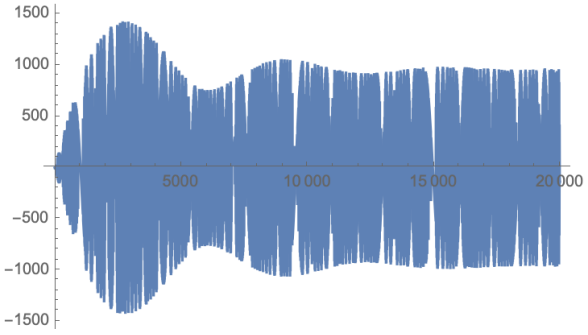

(b) In presence of losses and resonance. The initial conditions: $x(0) = 0, \dot{x}(0) = 0$. Set parameters : $\omega_0 = 0.5, \omega_{drv} = 0.501, A = 1, Q = 10^3$.

Figure 2: Solution $x(t)$ of equation 1. In fig.(a) it is in presence of the loss term. The trend of the peaks grows linearly in time until the damping time $\sim$ few $\times \frac{10^3}{0.5}$. After this value, the solution saturates around $x \sim 4Q$. In fig.(b) it is in presence of the loss term for non-resonance.

In the non-resonant case, $\omega_0 \neq \omega_{drv}$, we can see that changing the frequency of the source for a part over Q, the plot of the solution is completely stoned. We can find the analytic solution of equation (1) in the Fourier space. We find that $\tilde{x}(\omega_{drv})$ is a Lorenzian distribution centred in the characteristic frequency of the cavity ω_0, i.e.

$$\tilde{x}(\omega_{drv}) \propto \frac{1}{(\omega - \omega)^2 + (\omega_0/Q)^2} \tag{2}$$

where the FWHM is ω_0/Q and the half maximum is Q which is huge in SRF cavities. So the price to pay is that the Lorenzian is strongly ω_0-centered and narrow. Hence the frequencies of the GW that can be detected are GHz$(1 \pm 1/Q)$. Basically, for the order of Q, $\tilde{x}(\omega) \sim \delta(\omega - \omega_0)$. However, there is a technique called *scanning* which allows the distribution to move with translations in ω. When there is match between ω_{GW} and ω_0 within a part over Q, then we have detection !
The implementation of *scanning* for cavity detectors corresponds to press and insert physical objects inside the cavity in order to change the frequency ω_0. In fact $\omega_0 \sim \frac{\mathcal{O}(1)}{\text{length}}$ [1], so deforming the length of cavity or its geometry, the characteristic frequency changes.

The Quality Factor is a fundamental characteristic for the cavities. Indeed, it describes decay rate of excited mode m in cavity,

$$\frac{dP_m}{dt} = -\frac{\omega_m}{Q_m} P_m \ . \tag{3}$$

[1]There is another (stronger) interaction to consider, i.e. the *indirect interaction* of GW with boundary of the cavity.

Moreover, the typical parameters for Niobium cavity are : $T_c = 9.2$ K, $B_c = 0.2$ T, so that $Q \sim \mathcal{O}(10^{10})$. We can optimistically assume $Q \sim \mathcal{O}(10^{12})$.

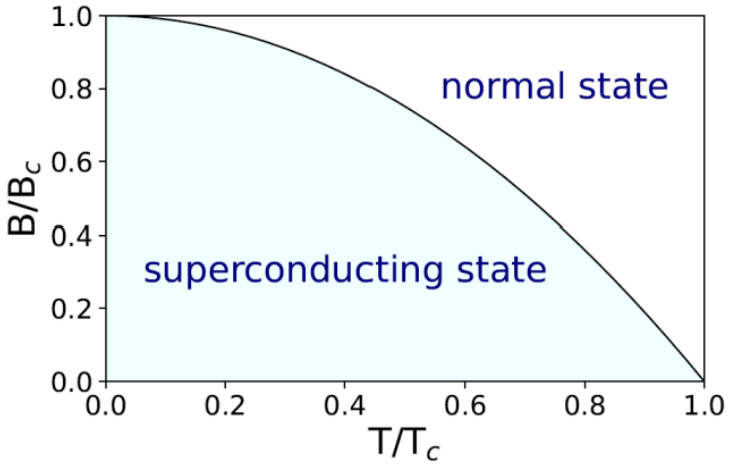

Figure 3: Diagram from W. Buckel, R. Kleiner, *Superconductivity*, John Wiley & Sons, Inc. (2004).

Until now, we imagined to approximate the SRF cavities like a HO with some losses. Of course, in the reality, the physics is more complicated. For instance we are not considering the nonlinearities of the cavity system. Recently nonlinear effect have been studied and shown to depend on both the disorder parameter and the temperature of the superconductor.

3 Gravitational Waves

The first direct observation of GW in 2016 by the ground-based interferometers LIGO and Virgo represented the irrefutable proof of Einstein's theory of General Relativity. These interferometers are able to detect GW in the Hz-kHz frequency range. The Universe is expected to be populated by GW over many decades in frequency, analogous to EM radiation, carrying information that may revolutionize our understanding of Nature. This fact has spurred the development of a large array of observational efforts with the aim of detecting much lower frequency signals compared to current interferometers. For this reason the detection with SRF cavities gives us the opportunity to explore another region of the spectrum of GW, i.e the GHz regime.

3.1 Expansion around flat space

In this subsection we derive the GW like a linear perturbation of a flat space. Indeed, the General Relativity, in this expansion and breaking the local invariance, can be thought like a Classical Field Theory in a flat space $\eta_{\mu\nu} = \mathrm{diag}(-1, 1, 1, 1)$ with a spin-2 field $h_{\mu\nu}$. The gravitational action is $\mathcal{S} = \mathcal{S}_{HE} + \mathcal{S}_M$, where

$$\mathcal{S}_{HE} = \frac{c^3}{16\pi G} \int d^4x \sqrt{-g} R \tag{4}$$

is the Hilbert-Einstein action and $\mathcal{S}_M$ is the action of the matter. With the action principle, making a variation of the curved metric, according to

$$\delta \mathcal{S}_M = \frac{1}{2c} \int d^4x \sqrt{-g} T^{\mu\nu} \delta g_{\mu\nu},$$

we find the Einstein equations,

$$R_{\mu\nu} - \frac{1}{2} g_{\mu\nu} R = \frac{8\pi G}{c^4} T_{\mu\nu}. \tag{5}$$

In General Relativity (GR) the *gauge symmetry* corresponds to the invariance under an arbitrary diffeomorphism : $x^\mu \to x'^\mu$. As a first step, we wish to study the expansion of the Einstein equations around the flat-space metric. We write

$$g_{\mu\nu} = \eta_{\mu\nu} + h_{\mu\nu}, \qquad |h_{\mu\nu}| \ll 1 \tag{6}$$

and we expand the equations of motion to linear order in h. The resulting theory is called *linearized theory*. The symmetry of this theory is described by the transformation $x^\mu \to x'^\mu = x^\mu + \xi^\mu$ where the derivatives $|\partial_\mu \xi_\nu|$ are at most of the same order of smallness as $|h_{\mu\nu}|$. If we transform the metric under diffeomorphism :

$$g_{\mu\nu}(x) \to g'_{\mu\nu}(x') = \frac{\partial x^\rho}{\partial x'^\mu}\frac{\partial x^\sigma}{\partial x'^\nu} g_{\rho\sigma}(x)$$

we find that the transformation of $h_{\mu\nu}$, to lowest order, is

$$h_{\mu\nu}(x) \to h'_{\mu\nu}(x') = h_{\mu\nu}(x) - (\partial_\mu \xi_\nu + \partial_\nu \xi_\mu)\ . \tag{7}$$

If $|\partial_\mu \xi_\nu|$ are at most of the same order of smallness as $|h_{\mu\nu}|$, the condition $|h_{\mu\nu}| \ll 1$ is preserved. The extension of Lorentz transformation is trivial : $h'_{\mu\nu}(x') = \Lambda_\mu^{\ \rho}\Lambda_\nu^{\ \sigma} h_{\rho\sigma}$, it shows that $h_{\mu\nu}$ is a tensor in the flat space. The rotations never spoil the condition $|h_{\mu\nu}| \ll 1$ while for the boosts we must limit ourselves to those that do not spoil the condition. Also under constant traslations the $h_{\mu\nu}$ is invariant. So, we can say that the linearized theory is invariant under Poincaré group. In contrast, the full General Relativity does not have Poincaré symmetry.

The Riemann tensor after this expansion, becomes

$$R_{\mu\nu\rho\sigma} = \frac{1}{2}(\partial_\nu\partial_\rho h_{\mu\sigma} + \partial_\mu\partial_\sigma h_{\nu\rho} - \partial_\mu\partial_\rho h_{\nu\sigma} - \partial_\nu\partial_\sigma h_{\mu\rho}) \tag{8}$$

and we can see that it is invariant under transformation (7). Defining $\bar{h}_{\mu\nu} = h_{\mu\nu} - 1/2\eta_{\mu\nu}h$ where h is the determinant and $\bar{h} = -h$, we can find the linearized Einstein equations :

$$\Box \bar{h}_{\mu\nu} = -\frac{16\pi G}{c^4} T_{\mu\nu} \tag{9}$$

where we used the gauge freedom to chose the *Lorentz gauge*,

$$\partial^\nu \bar{h}_{\mu\nu} = 0\ . \tag{10}$$

It is interesting to note from (9) that, outside the source ($T_{\mu\nu} = 0$), the GW travels at the speed of light. Indeed, equation (9) is a D'Alembert wave equation in presence of a source. As we can see from equation (8), $h_{\mu\nu}$ has Riemann tensor not null. It means that the GWs are waves of curvature of space-time. In Appendix A we reported a deeper analysis of the two possible frames we can choose for GWs : *TT frame* and *proper detector frame*. We will work in the second one which is physically the frame of Lab and which generalizes the notion of an inertial observer to curved space-time and reduces to the flat space-time metric in the $\omega_g \to 0$ limit. We can do that if the condition $\lambda_g \gg L_{det}$, where λ_g is the wavelength and L_{det} the characteristic length of the detector, is preserved.

3.2 Graviton-photon interaction

In this subsection we want to translate the graviton - photon interaction in the language of classical fields. The GR-EM coupling is encapsulated in the Einstein-Maxwell action

$$\mathcal{S} = -\frac{1}{4}\int d^4x\sqrt{-g}g^{\mu\alpha}g^{\nu\beta}F_{\mu\nu}F_{\alpha\beta} \tag{11}$$

where $F_{\mu\nu}$ is the EM field strength. We linearize the theory for isolating the effect of GW, i.e. $g_{\mu\nu} = \eta_{\mu\nu} + h_{\mu\nu} + \mathcal{O}(h^2)$, and we keep only the $\mathcal{O}(h)$ terms. We find $\mathcal{S} \propto \int hF^2$. Therefore the Feynmann diagram associated is a vertex with two photons and the graviton. Schematically the form of interaction scales like $\sim h\mathbf{B} \cdot \mathbf{B}_0$, where $\mathbf{B}_0$ is the static B-field controlled in the Lab by us and $\mathbf{B}$ the B-field to read out. This implies that a GW of frequency ω_g can generate an EM field of typical magnitude $h\mathbf{B}_0$ at the same frequency. Inside an EM cavity, this signal will ring up coherently if ω_g matches the cavity's resonant frequency. At the level of single quanta, this effect can be interpreted as graviton-photon mixing in a background magnetic field, known as the inverse-Gertsenshtein effect. The original Gertsenshtein effect, discovered in 1962, comes from $\Box h_{\{+,\times\}} = 16\pi G B_0 \partial_i A\{+,\times\}$.

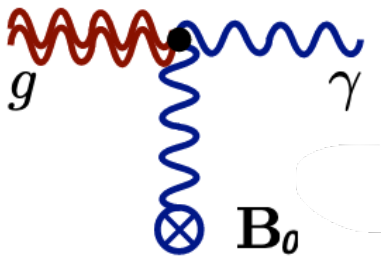

Figure 4: Diagram of inverse-Gertsenshtein effect.

This kind of effect can be described also at a classical level, using the formalism of *effective* current. When the cavity size is of order $L_{det} \sim 1/\omega_g$, the effect of interaction produces a $j_{\text{eff}} \sim \omega_g h B_0 \sim \mathcal{O}(h)$. The direction of this current is not determined by the polarization of the GW, being the graviton a spin-2 tensor field with a gauge freedom. We report below a figure which illustrates the effective conversion of a GW into and classical current (from the Berlin et al.'s paper [4]).

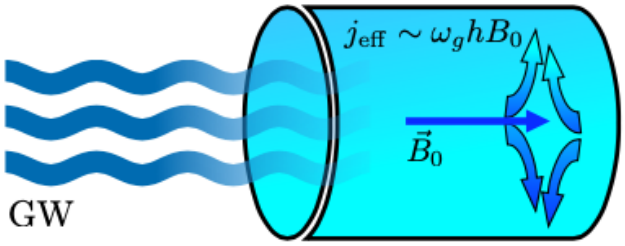

Figure 5: Figurative representation of GW - j_{eff} conversion.

This is a good method to detect GWs. We note that it is already well established in axion experiments (e.g. ADMX). The equation of motion can be derived directly from the action (11). Linearizing the theory and integrating by parts we find the following $\mathcal{O}(h)$ term in the action

$$\mathcal{S}[\mathcal{O}(h)] = -\frac{1}{2}\int d^4x j^{\mu}_{\text{eff}} A_{\mu} \tag{12}$$

where the effective 4-current is

$$j^{\mu}_{\text{eff}} \equiv \partial_{\nu}\Big(\frac{1}{2}hF^{\mu\nu} + h^{\nu}{}_{\alpha}F^{\alpha\mu} - h^{\mu}{}_{\alpha}F^{\alpha\nu}\Big) \tag{13}$$

which is not a true 4-current. Indeed, it is not invariant under transformations between frames. By the way, let's analyze the electromagnetism in presence of the linearized gravity. We have just

to substitute the derivative with the covariant derivative ∇_μ in order to find the GW-Maxwell's equations.

$$\nabla_\mu F^{\mu\nu} = -\frac{4\pi}{c} J^\nu, \qquad \nabla_{[\mu} F_{\nu\rho]} = 0 \,. \tag{14}$$

Now, expanding the covariant derivative and the metric around the space, we find

$$\partial_\mu F^{\mu\nu} \simeq J^\nu \Big(1 + \frac{h_\alpha^{\ \alpha}}{2}\Big) - h^{\nu\alpha} J_\alpha + \frac{\partial_\mu \Big(h_\alpha^{\ \alpha} F^{\mu\nu}\Big)}{2} + \partial_\mu (h^{\mu\alpha} F_\alpha^{\ \nu} + h^{\nu\alpha} F_\alpha^{\ \mu}) \,. \tag{15}$$

So, we see that a variations of metric (GWs) acts as EM source terms.

A GW can be most easily described in the TT-gauge

$$\partial_\mu h^{\mu\nu} = 0, \qquad h_\mu^{\ \mu} = 0, \qquad h_{00} = h_{0i} = 0 \,. \tag{16}$$

The Riemann tensor is gauge invariant and it can be computed in the TT-guage, i.e.

$$R_{0i0j} = -\frac{1}{2} \ddot{h}_{ij}^{TT} \,. \tag{17}$$

For instance, a monochromatic GW in the z-direction can take the simple form

$$h_{\mu\nu}^{TT} = H_{\mu\nu} e^{i\omega(t-z)}, \qquad H_{\mu\nu} = \begin{pmatrix} 0 & 0 & 0 & 0 \\ 0 & h_+ & h_\times & 0 \\ 0 & h_\times & h_+ & 0 \\ 0 & 0 & 0 & 0 \end{pmatrix} . \tag{18}$$

However, the TT-frame is *not* physical! It does not describe a Gravitational Wave as seen by a local observer. Therefore, we should make another gauge choice. A better choice is the Fermi Normal Coordinates.

Fermi Normal Coordinates (FNC) are defined in the vicinity of a time-like geodesic G in a curved manifold $\mathcal{M}$. The coordinate system (t, x_i) is constructed so that geodesic is at zero spatial coordinates $x_i|_G = 0$. The metric is Minkowski along the geodesic, $g_{\mu\nu}|_G = \eta_{\mu\nu}$, i.e. the spacetime is flat and the Riemann tensor is locally zero along the geodesic. Moreover the first derivatives vanish along the geodesic, i.e. $\partial_\lambda g_{\mu\nu}|_G = 0$. In summary, the FNC are the inertial coordinates that a free-falling observer would set in a neighborhood around them, not just at one instant in time but all along their world-line.

The general form of metric in the FNC is still complicated even if we consider the following simplification : $\mathrm{a} = 0$ and $\omega = 0$. It is justified by the fact that the Gravitational field of the Earth is almost static and varies on typical frequencies $\lesssim 0.1$ Hz. So, for convenience, we can thus choose to evaluate the Riemann tensor in TT frame. In this case we find

$$\begin{aligned}
h_{00} &= -\omega_h^2 h_{ab}^{TT} x^a x^b \Big[-\frac{i}{\omega_g z} + \frac{1 - e^{-i\omega_g z}}{(\omega_g z)^2} \Big] \\
h_{ij} &= \omega_g^2 \Big[(\delta_{ij} h_{ja}^{TT} + \delta_{jz} h_{ia}^{TT}) z x^a - h_{ij}^{TT} z^2 - \delta_{iz}\delta_{jz} h_{ab}^{TT} x^a x^b \Big] \Big[-\frac{1 + e^{-i\omega_g z}}{(\omega_g z)^2} - 2i \frac{1 - e^{-i\omega_g z}}{(\omega_g z)^3} \Big] \\
h_{0i} &= -\omega_g^2 (h_{ia}^{TT} z x^a - \delta_{iz} h_{ab}^{TT} x^a x^b) \Big[-\frac{i}{2\omega_g z} - \frac{e^{-i\omega_g z}}{(\omega_g z)^2} - i \frac{1 - e^{-i\omega_g z}}{(\omega_g z)^3} \Big] ,
\end{aligned} \tag{19}$$

where the GW is evaluated in the spatial origin, the indices $a, b = x, y$ run over the perpendicular components to the GW's direction of propagation. Substituting the expression above into (13) we find the effective current inducted by the GW in the cavity in presence of a static B-field, in terms of the TT polarizations $(+, \times)$.

3.3 SRF cavities for GW detection

For this report we consider cylindrical cavities that admits analytic expressions for the cavity modes. Moreover if $\mathbf{B}_0$ is aligned along the symmetry axis of the cavity, hence the considerations of EM signal become easier. The general idea to detect GWs with cavities comes from two possible interactions : the *direct* interaction of the GW with the EM field inside the cavity and the *indirect* or mechanical interaction of the GW with the boundaries of the cavity. First of all, let's focus on the first of these. In the so called *Heterodyne Experiments*, the GW is on-resonant with the frequency difference of two cavity modes and couples to both E- and B-field. Because of $L_{cav} \sim 1/\omega_0$, it is difficult to build a cavity as a detector in low frequencies regime. Therefore, the Heterodyne protocol is a good technique to overcome this problem.

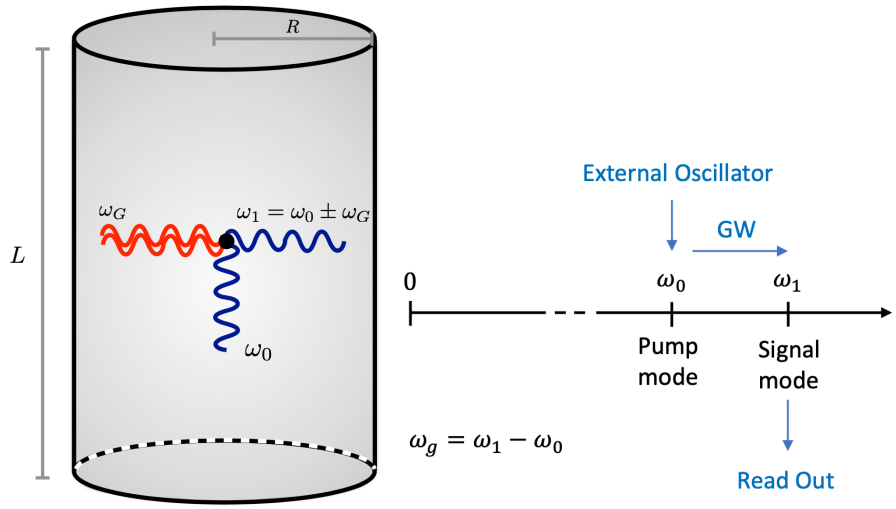

(a) The inverse-Gertsenshtein interaction

(b) Schematic example HD experiment.

We can use an external oscillator in the *pump* mode of frequency ω_0 and let's call ω_1 the frequency of the read-out mode. The GW is going to be on-resonant with $\Delta\omega = |\omega_1 \pm \omega_0|$. For SRF cavity ($\omega \sim$ GHz) with $Q_{int} \sim 10^9 \div 10^{13}$, the tunability is $\delta\omega \sim$ MHz.

The other interaction comes from the deformation of the cavity and hence the resonant frequency of that. In this case, the GW is source of an additional vibrational signal. Indeed the GW perturbs the cavity wall Δx and since the cavity modes depend on the geometry, the frequency will change like $\omega_0 \to \omega_0(1 + f(\Delta x))$. In the proper detector frame, the effect of GW is that of Newtonian force on the test mass, $F_i \simeq \frac{m}{2}\ddot{h}^{TT}_{ij}x^j$. In few words, the passing gravitational wave will move walls, spreading power in frequency space.

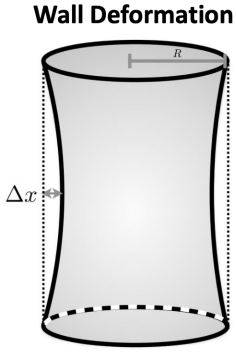

Figure 6: Deformation of the cavity by the passage of a GW.

As we saw above, we need to calculate the electromagnetic signal that arises in the resonant cavity immersed in the static B-field $\mathbf{B}_0$ which is also spatially uniform in *proper detector* frame. Let's have a general discussion on the structure of the read-out EM signal for any SRF cavity. Assume for a moment that this cavity permits a decomposition of the electromagnetic field into their resonant modes. For the general formalism, we follow the Ref. [4] which is an extension of Axion with SRF cavities (Ref. [10]) to GW detection.

The components of the effective current $j^{\mu}_{\rm eff} = (\rho_{\rm eff}, \mathbf{j}_{\rm eff})$ have to be added to the inhomogeneous Maxwell's equations,

$$\begin{aligned} \nabla \cdot \mathbf{E} &= \rho_{\rm eff} + \rho \\ \nabla \times \mathbf{B} - \partial_t \mathbf{E} &= \mathbf{j}_{\rm eff} + \mathbf{j} \end{aligned} \tag{20}$$

where ρ and $\mathbf{j}$ are the physical charge and current. We identify $\mathbf{B}_0$ (the static external B-field) like that piece of $\mathbf{j}$ which doesn't depend on $h_{\mu\nu}$, so that $\nabla \times \mathbf{B}_0 = \mathbf{j}_0$. We are interested to the terms of order $\mathcal{O}(h)$. The reader can see the Ref. [4] for the proof that the homogeneous Maxwell's equations ($\nabla \cdot \mathbf{B} = 0, \nabla \times \mathbf{E} + \partial_t \mathbf{B} = 0$) are not affected by the GW. The deep reason is that these Maxwell's equations come from a topological metric independent equation of motion, $dF = 0$, where d is the exterior derivative and F a two (differential) form. It is important to note that the homogeneous equations determine the resonant cavity modes. Combining the second equation of (20) and the Faraday's law, we find

$$\nabla \times \nabla \times \mathbf{E} + \partial_t^2 = -\partial_t \mathbf{j}_{\rm eff} - \partial_t \mathbf{j} \, . \tag{21}$$

The electric field inside the cavity can be expanded in terms of the resonant modes $\mathbf{E}_n$:

$$\mathbf{E}(\mathbf{x}, t) = \sum_n e_n(t) \mathbf{E}_n(\mathbf{x}) \tag{22}$$

where e_n is a dimensionless time-dependent coefficient. We assume to consider only solenoidal and non-solenoidal (not considering the irrotational modes) contributions. The spatial $\mathbf{E}_n$ functions satisfy the relations:

$$\begin{aligned} \nabla^2 \mathbf{E}_n(\mathbf{x}) &= -\omega_n^2 \mathbf{E}_n(\mathbf{x}) \\ \int_V d^3\mathbf{x} \mathbf{E}_n(\mathbf{x}) \cdot \mathbf{E}_m(\mathbf{x})^* &= \delta_{nm} \int_V d^3\mathbf{x} |\mathbf{E}_n(\mathbf{x})|^2 \end{aligned} \tag{23}$$

where ω_n is the resonant frequency of the n-mode of the cavity and V is the cavity's volume. Another constrain that the modes satisfy is $\hat{\mathbf{n}} \times \mathbf{E}_n(\mathbf{x}) = 0$. The boundary of the cavity can oscillate in the presence of the GW which induce the tidal force that will affect our signal at $\mathcal{O}(h^2)$. Combining the equations (22)-(23), we can write the wave equation in terms of the coefficients e_n, i.e.

$$\left(\partial_t^2 + \frac{\omega_n}{Q_n} \partial_t + \omega_n^2 \right) = -\frac{\int_V d^3\mathbf{x} \mathbf{E}_n^* \cdot \partial_t \mathbf{j}_{\rm eff}}{\int_V d^3\mathbf{x} |\mathbf{E}_n|^2} \tag{24}$$

where the quality factor Q_n appears from the losses of the cavity. The parameters which are affected by the interaction between the GW and the cavity walls are ω_n and V, i.e. $\mathcal{O}(V, \omega_n) \sim \mathcal{O}(h)$ .Therefore, from (24) we see that the effect of GW is $\mathcal{O}(he_n)$ and $\mathcal{O}(hj_{\rm eff})$, hence both of order $\mathcal{O}(h^2)$. For a monochromatic GW on resonance with the cavity mode ($\omega_g \simeq \omega_n$), $\mathbf{j}_{\rm eff}(\mathbf{x}, t) = e^{i\omega_g t} \mathbf{j}_{\rm eff}(\mathbf{x})$, the solution of (24) is simplified by the large quality factor. Therefore, taking the stationary solution of that equation, we find analytically :

$$\mathbf{E}_{\rm sig}(\mathbf{x}, t) = e_n \mathbf{E}_n = -\frac{\int_V d^3\mathbf{x}' \mathbf{E}_n^* \cdot \mathbf{j}_{\rm eff}}{\int_V d^3\mathbf{x}' |\mathbf{E}_n|^2} \frac{Q_n}{\omega_g} \mathbf{E}_n(\mathbf{x}) e^{i\omega_g t} \, . \tag{25}$$

For more details the reader can see Ref. [4]. Here it's sufficient to show that electric field to read-out is proportional to Q_n which is huge for SRF cavities. Some results and formulas will be presented below when necessary.

As we said above, the effective current sources a small signal field $B_{\rm sig} \sim hB_0$. Typically, the signals are classified into two different categories : stochastic GW backgrounds and GWs with a preferred direction of propagation and well defined frequency. We concentrate on the latter case. The setup we imagine is reported in Figure 7 where a GW can interact with the static B-field of the cavity and excite a specific cavity mode ($\omega_{\rm sig} \simeq \omega_g \sim$ GHz)[2].

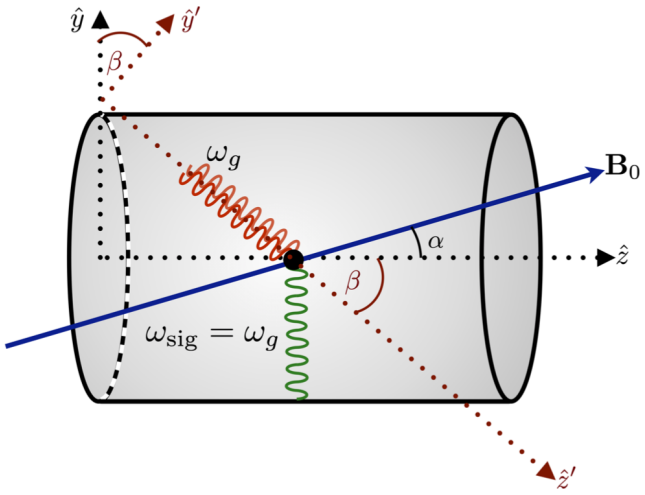

Figure 7: Interacting GW (red) with the static B-field (blue) resonantly exciting a cavity mode (green).

Still following the Ref. [4], the sensitivity of the above setup to the GW strain h is

$$h \gtrsim 2 \times 10^{-22} \times \left(\frac{1\ \text{GHz}}{\omega_g/2\pi}\right)^{3/2} \left(\frac{0.1}{\eta_n}\right) \left(\frac{8\ \text{T}}{B_0}\right) \left(\frac{0.1\ \text{m}^3}{V}\right)^{5/6} \left(\frac{10^5}{Q}\right)^{1/2} \times \left(\frac{T_{\rm sys}}{1\ \text{K}}\right)^{1/2} \left(\frac{\Delta\nu}{10\ \text{kHz}}\right)^{1/4} \left(\frac{1\ \text{min}}{t_{\rm int}}\right)^{1/4} \tag{26}$$

where η_n is the coupling coefficient[3] of the cavity, $T_{\rm sym}$ the system temperature, $\Delta\nu$ the signal bandwidth and $t_{\rm int}$ the integration time. In Figure 8 it is shown the sensitivity of the cavity experiment, originally thought to detect Axion DM.

[2]In Appendix B the reader can find a summary of the sources of GW in the spectrum regime kHz - GHz.

[3]In the sensitivity estimate it is defined as

$$\eta_n \equiv \frac{\left|\int_V d^3\mathbf{x}\mathbf{E}_n^* \cdot \hat{\mathbf{j}}_{+,\times}\right|}{V^{1/2}(\int_V d^3\mathbf{x}|\mathbf{E}_n|^2)^{1/2}}$$

where $\hat{\mathbf{j}}_{+,\times}$ is the effective current inducted by GW depending on the polarization.

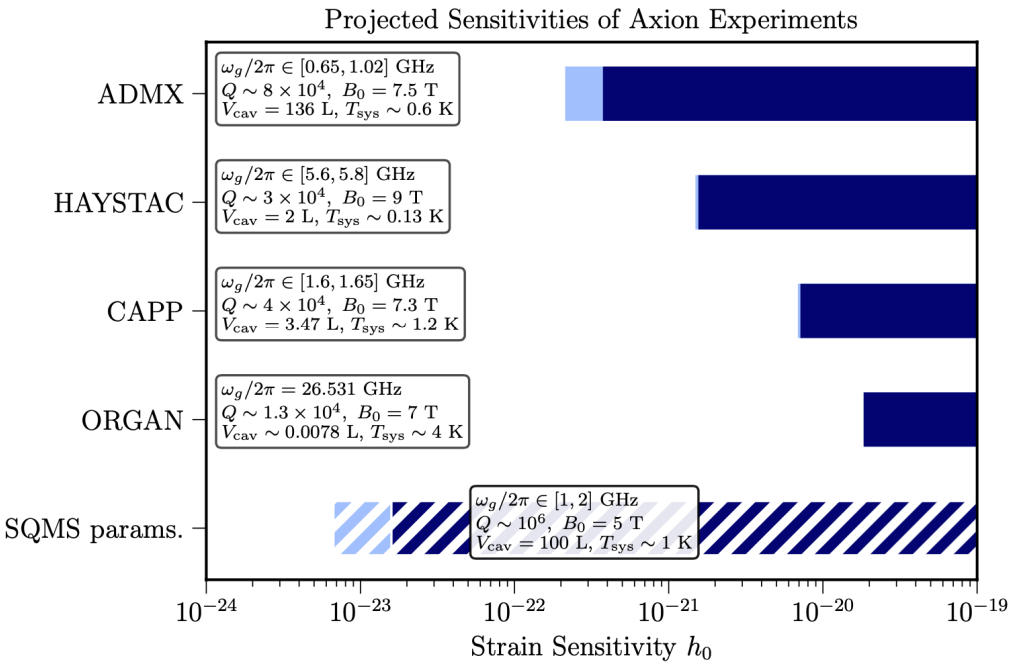

Figure 8: The projected sensitivity of axion cavity haloscope experiments to high-frequency coherent gravitational waves. From [4].

The resonant cavities operate in regime where the GW frequency is comparable to the inverse geometric size of the cavity, $\omega_g L \sim 1$.

From Figure 4 which describes the *electromagnetic* interaction of the GW, we see that the $\mathbf{B}_0$ field can be static or oscillating. The effects to the $B_{\rm sig}$ are different in these two cases.

- $\Delta B_{\rm sig} \sim h B_0 \sqrt{Q} \min\left[\frac{\omega_g^2}{\omega_0^2}, 1\right]$ for the oscillating case.
- $\Delta B_{\rm sig} \sim h B_0 \sqrt{Q} \min\left[\frac{\omega_g^2}{\omega_0^2}\frac{\omega_g}{\omega_0}, 1\right]$ for the static case.

The suppressive terms $\sim \frac{\omega_g^2}{\omega_0^2}$ come form the Riemann tensor which contains the second derivatives of the GW. For the static case also the time derivative of the current contributes. From this parametric argument it is not obvious which of these effects has a best sensitivity. We could prove that the oscillating case "wins". While, the mechanical interaction has not a suppressive factor because the resonant frequency can be lower than the GW frequency. At the level of single quanta, the interaction is a vertex with a phonon-GW-photon. The variation of the B-field (photon in the vertex) is

- $\Delta B_{\rm sig} \sim h B_0 \sqrt{Q}$.

3.4 Noise and Sensitivity

In this subsection, we want briefly to describe the expected dominant noise sources for the setup, schematically shown in Figure 9.

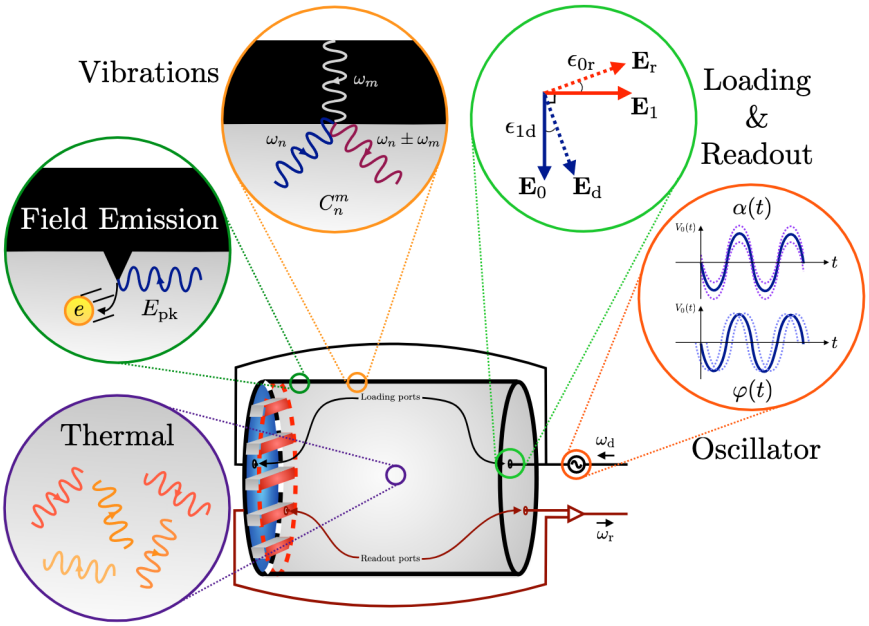

Figure 9: A diagram of the all sources of noise for the electromagnetic signal to readout in presence of static B-field.

The two main sources of noise are: the oscillator phase noise and the mechanical noise. Increasing the quality factor, other than increasing the signal power, decreases these two sources of noise. Following Ref. [10], we can find that the power spectral density for the oscillator phase noise is

$$S_{\rm phase}(\omega) \simeq \frac{1}{2}\epsilon_{1d}^2 \underbrace{S_\phi(\omega-\omega_0)}_{\text{Input Oscillator}} \underbrace{\frac{(\omega\omega_1/Q_1)^2}{(\omega^2-\omega_1^2)^2+(\omega\omega_1/Q_1)^2}}_{\text{Cavity response (B−W)}} \underbrace{\frac{\omega_0 Q_1}{\omega_0 Q_0} P_{\rm in}}_{\text{Overall Normalization}} \tag{27}$$

where ϵ_{1d} is the small coupling of the oscillator to the signal mode. From the MAGO's setup of '05 $\epsilon \simeq 10^{-7}$. The other important source of noise is the vibrations. So the mechanical power spectral density in this case can be written like

$$S_{\rm mech}(\omega) = \sum_{n=0,1} S_{\rm mech}^{(n)}(\omega) \simeq \frac{\epsilon_{1d}^2}{4}\frac{\omega_0}{Q_0}P_{\rm in}$$

$$\sum_{n=0,1} \underbrace{\frac{\overbrace{(S_{q_m}(\omega-\omega_0)}^{\text{Wall Displacement}}/V^{2/3})(\omega_n/Q_n)\omega_n^4\omega^2}{\Big[(\omega^2-\omega_n^2)^2+(\omega\omega_n/Q_n)^2\Big]\Big[(\omega_0^2-\omega_n^2)^2+(\omega_0\omega_n/Q_n)^2\Big]}}_{\text{Cavity Response}} \tag{28}$$

where the sum is over the pump ($n=0$) and signal ($n=1$) modes. $S_{q_m}(\omega-\omega_0)$ is the spectrum of vibrations which can be measured by MAGO and DarkSRF in the spectrum we care about. The other sources of noises described by PDSs are

- Thermal Noise (cavity walls)

$$S_{th}(\omega) = \frac{Q_1}{Q_{int}}\frac{4\pi T k_B(\omega\omega_1/Q_1)^2}{(\omega^2-\omega_1^2)^2+(\omega\omega_1/Q_1)^2}$$

- Amplifier Noise

$$S_{ql}(\omega) = 4\pi\hbar\omega_1$$

All PSDs can be summed up and we find

$$S_{noise}(\omega) = S_{ql}(\omega) + \frac{Q_1}{Q_{cpl}}\Big(S_{th}(\omega) + S_{phase}(\omega) + S^{(1)}_{mech}(\omega)\Big) + \frac{Q_0}{Q_{cpl}} S^{(0)}_{mech}(\omega) \tag{29}$$

which describes the total source of noise for the read-out signal. For more details about the other sources of noise, the reader can see Ref. [10]. Only for completeness we report below the comparison of different noise powers.

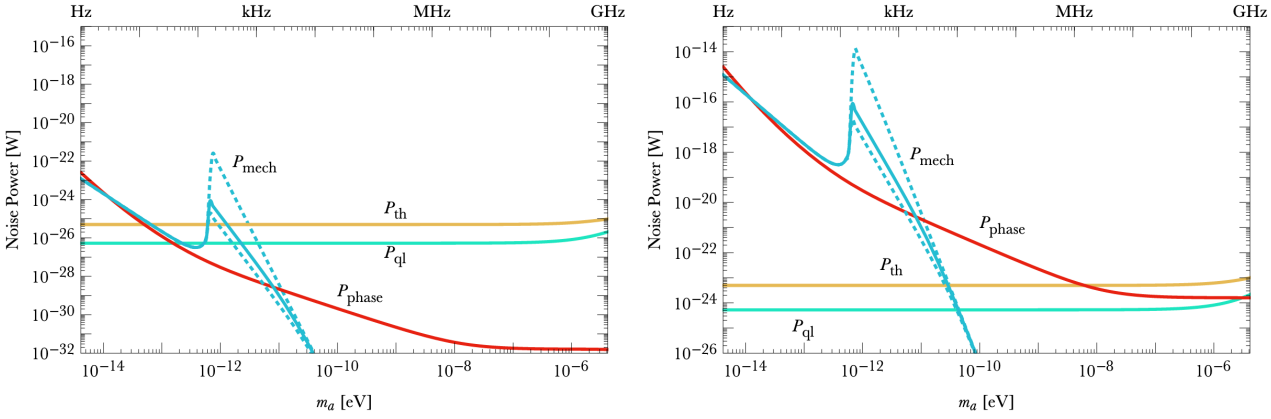

(a) $\epsilon_{\rm 1d} = 10^{-7}$, $Q_{\rm int} = 10^{12}$ (b) $\epsilon_{\rm 1d} = 10^{-5}$, $Q_{\rm int} = 10^{10}$

Figure 10: Comparison of the total power in thermal (yellow), amplifier (cyan), oscillator phase (red), and mechanical vibration (blue) noise, shown as a function of the axion mass m_a. Here the frequency $= m_a/2\pi$. It is just a parameterization in frequency.

The two plots are linked to the values of parameters ϵ and Q used recently in different experiments. We can note that in the regime of MHz the $P_{\rm ph}$ decreases and the thermal source is the dominant one (see figure (a)). This the reason why in the computation of the signal-to-noise ratio (SNR[4]) we can consider like $\delta P_{\rm noise}$ the thermal power $P_{\rm th}$. From the Dicke Radiometer equation it is known that

$$\text{SNR} \sim \frac{P_{\rm sig}}{T}\sqrt{\frac{t_{\rm int}}{\Delta\omega}} \tag{30}$$

where $\Delta\omega = \omega_0/Q$.

3.5 Cavity - qubit system for GW detection

The first natural question we should ask ourselves is if the sensitivity of GW measurements increases adding a qubit inside the cavity. Moreover, to understand that, it is also necessary to think about the direct interaction between the GW and the qubit itself (see subsection 3.6 below). The conjecture is that the presence of the qubit changes the SNR of a factor larger than one,

$$\text{SNR} \to \text{SNR} \times \sqrt{\frac{T_{\rm cav}}{T_{\rm R}}} \tag{31}$$

where $T_{\rm R}$ is the temperature of the readout mode. The qubit seems to reduce the read-out noise.

Before to explain what we understood or didn't about the direct interaction GW-qubit yet, it is important to say how nowadays the qubits are used for detection of new particles. The integration of a qubit into an ultra high cavity may allow for employing a photon counting non-demolition measurement for DM searches. The qubit has just the role of instrument for parity measurement in the number of resonant photons in the cavity.

[4] $\text{SNR} \sim \dfrac{P_{\rm sig}}{\delta P_{\rm noise}}$

3.6 GW - qubit direct interaction

It is hard to find a way to match the linearized theory of General Relativity, i.e. the GWs, with the quantum theory of qubit states. The personal idea of the author of this report is to find a mapping between the spinor field of the QED for a fermion spin-1/2 in the chiral representation and the two level states of the qubit. The mathematical work consists of finding this formal mapping between these two worlds. The symmetries of QFT should be mapped to some operators in the Hilbert space of the qubit. For instance, the Charge Conjunction is mapped into the Pauli matrix σ_y while the Parity transformation is mapped into the Pauli matrix σ_x.

The spinor field ψ_α, where $\alpha = 1, \dots, 4$ is the spinorial index, can be written in the chiral representation,

$$\psi = \begin{pmatrix} \psi_R \\ \psi_L \end{pmatrix}, \quad \gamma^0 = \begin{pmatrix} 0 & 1 \\ 1 & 0 \end{pmatrix}, \quad \gamma^i = \begin{pmatrix} 0 & -\sigma^i \\ \sigma^i & 0 \end{pmatrix}, \quad \gamma^5 = \begin{pmatrix} 1 & 0 \\ 0 & -1 \end{pmatrix} \tag{32}$$

and the mapping consists of $\psi_R \mapsto |0\rangle, \psi_L \mapsto |1\rangle$. The full density Lagrangian of QED in presence of *dipole* interaction is

$$\mathcal{L} = -\frac{1}{4} F_{\mu\nu} F^{\mu\nu} + \bar{\psi}(i\partial\!\!\!/ - m)\psi \underbrace{- e\bar{\psi}\gamma^\mu A_\mu \psi}_{\text{(a)}} + \underbrace{\Lambda \bar{\psi}\sigma^{\mu\nu}\gamma^5 \psi F_{\mu\nu}}_{\text{(b)}}, \tag{33}$$

where $\sigma^{\mu\nu} = \frac{i}{2}(\bar{\sigma}^\mu \sigma^\nu - \bar{\sigma}^\nu \sigma^\mu)$. We can show that the only term which couples the left with the right handed part is the the interaction term (b). Indeed, expanding the calculation in the chiral representation, we find

$$\begin{aligned} \Lambda \bar{\psi}\sigma^{\mu\nu}\gamma^5 \psi F_{\mu\nu} &= \Lambda(\psi_R^\dagger, \psi_L^\dagger) \begin{pmatrix} 0 & 1 \\ 1 & 0 \end{pmatrix} \sigma^{\mu\nu} \begin{pmatrix} 1 & 0 \\ 0 & -1 \end{pmatrix} \begin{pmatrix} \psi_R \\ \psi_L \end{pmatrix} F_{\mu\nu} \\ &= \Lambda(\psi_L^\dagger, \psi_R^\dagger)\sigma^{\mu\nu} \begin{pmatrix} \psi_R \\ -\psi_L \end{pmatrix} \eta_{\mu\alpha} h_{\nu\beta} F^{\alpha\beta} + \dots \\ &\propto \Lambda(\psi_L^\dagger \psi_R - \psi_R^\dagger \psi_L)\eta_{\mu\alpha} h_{\nu\beta} F^{\alpha\beta} + \dots \end{aligned} \tag{34}$$

So, the interaction term produces a vertex with a GW, a photon (the signal reproducible in the Lab) and the mapped qubit. Therefore, we can see that the interaction with the qubit is allowed only in presence of a EM field in the background. In Figure 11 it is illustrated the vertex of interaction.

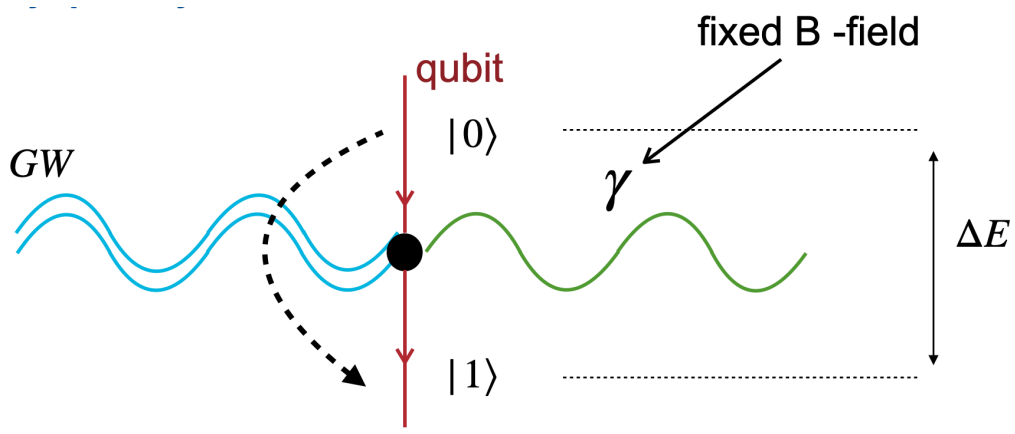

Figure 11: Interaction GW - qubit - photon

Ideally, if we fix the EM field in the Lab and the qubit initialized in the $|0\rangle$ state, if the GW couples, hence the qubit could flip into the excited state. This picture is obviously naive but it gives the physical idea of this interaction mapping.

3.7 Electron dipole interaction with gravity

Let's consider the spinor QED densitu Lagrangian for an electron which includes the kinetic term, the normal photon interaction term and the dipole magnetic term.

$$\mathcal{L} = \bar{\psi}(i\partial\!\!\!/ - m)\psi - e\bar{\psi}\gamma^{\mu}A_{\mu}\psi + g\bar{\psi}\sigma^{\mu\nu}\psi F_{\mu\nu} \tag{35}$$

If we calculate the equation of motion for the electron and we do the non-relativistic limit considering the external potential so much smaller than the electron mass, then we find the a Schrödinger equation with the Pauli Hamiltonian plus a dipole contribution,

$$H = \frac{1}{2m}(\mathbf{p} - e\mathbf{A})^2 + \frac{e}{2m}\boldsymbol{\sigma}\cdot\mathbf{B} - 2g(i\mathbf{E} + \mathbf{B})\cdot\boldsymbol{\sigma}\ . \tag{36}$$

What happens if we consider the expanded metric too?

$$\begin{aligned}
\bar{\psi}\sigma^{\mu\nu}g_{\mu\alpha}g_{\nu\beta}F^{\alpha\beta}\psi \approx\ & g\bar{\psi}\sigma^{\mu\nu}h_{\mu\alpha}\eta_{\nu\beta}F^{\alpha\beta} \\
\approx\ & g\bar{\psi}\Big[-2(E^i + B^i)h_{ij}\sigma^j + (B_k + E_k)\epsilon^{kij}h_{0i}\sigma_j + \\
+\ & i\sigma^j h_{00}E_j - \sigma^k h^j_j B_k\Big]\psi
\end{aligned} \tag{37}$$

Therefore, the magnetic dipole correction due to gravity coupling is

$$\mathbf{B}\cdot\boldsymbol{\sigma} \to B^i h_{ij}\sigma^j + B_k\epsilon^{kij}h_{0i}\sigma_j - \sigma^k h^j_j B_k\ . \tag{38}$$

This effect is so small to be observed with the current detectors. From equation 1.87 of Ref. [7] we can see that the metric in the laboratory frame is parametrically $h \sim x^2 R$, where x is the size of your detector and the Riemann tensor is related to the metric in the TT frame by $R \sim \omega^2 h_{TT}$, which gives $h \sim (x\omega)^2 h_{TT}$.

4 Dark Photon

It has been hypothesized that the dark photon exists as a new gauge boson It is dark because it results from a symmetry of a fictitious dark sector made up of particles that are fully neutral with respect to interactions in the Standard Model. Despite being dark, this new gauge boson can be found thanks to kinetic mixing with a regular, visible photon. In this section we describe briefly the theory of the dark photon and the Dixit's experiment Ref. [6] extended to the SQMS cavities. We also are going to show why there is not advantage to use Fock states of multi-photons for detection of dark photons.

In the last few years it is growing the hope of *dark sectors* in the Standard Model & and Beyond theory of particles. These sectors are called dark because the belonging particles are not charged under the Standard Model gauge groups. The dark sector is assumed to exist as a world parallel to our own.

4.1 Theory

The visible photon is assumed to be a gauge boson of the $U(1)$ gauge group of electromagnetism, i.e.the QED, while the dark photon comes to be identified as the boson of an extra $U(1)'$ symmetry[5]. The extended Standard Model gauge group is $SU(3) \times S(2) \times U(1) \times U(1)'$. Unlike the its SM counterpart, the dark photon is massive and this breaks the $U(1)'$ symmetry. The only renormalizable interaction one can write involving the dark photon field is a *kinetic* mixing with the SM photon. Therefore, the Lagrangian is

$$\mathcal{L} = \mathcal{L}_{SM} - \frac{1}{4} F'_{\mu\nu} F'^{\mu\nu} + \frac{1}{2} m^2_{A'} A'_\mu A'^\mu + \epsilon F^{\mu\nu} F'_{\mu\nu} \tag{39}$$

where ϵ is the kinetic coupling. The ordinary photon couples only to ordinary matter and the massive dark photon is characterized by a direct coupling to the electromagnetic current of the the SM particles (in addition to that to dark-sector matter) and described by the Lagrangian,

$$\mathcal{L} \supset -\frac{e\epsilon}{\sqrt{1-\epsilon^2}} J_\mu A'^\mu \simeq -e\epsilon J_\mu A'^\mu \,. \tag{40}$$

This is the choice defining the massive dark photon. The interaction between the dark photon and the visible photon is linear, $\mathcal{L}_{int} \propto -e\epsilon J^{EM}_\mu A'^\mu$. Therefore the diagram of interaction is that reported in Figure 12.

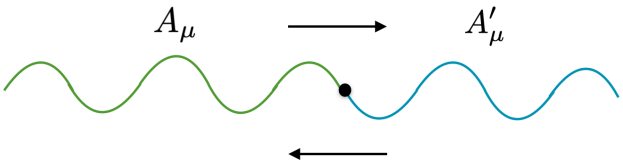

Figure 12: Interaction dark photon - visible photon.

The effect of a dark photon incoming to a cavity is independent from the electromagnetic field inside the cavity. We can parametrize this effect with an effective current as we did above for GWs. In particular, the effective current is

$$\mathbf{j}_{\text{eff}} \sim \epsilon m_{A'} \mathbf{A} \sim \epsilon m_{A'} \sqrt{\rho_{DM}} \hat{\mathbf{n}}_{A'} \tag{41}$$

where in the last step we use $m^2_{A'} A'^2 \sim \rho_{DM}$ in the non-relativistic limit. The density of DM in the universe is $\rho_{DM} \simeq 0.4$ GeV$/c$m^3.

In the following figure we report the projected sensitivity of the proposed search for dark photon dark matter with SQMS system assuming a fixed scan rate.

[5]We use the prime as sign to indicate the gauge group for the dark photon.

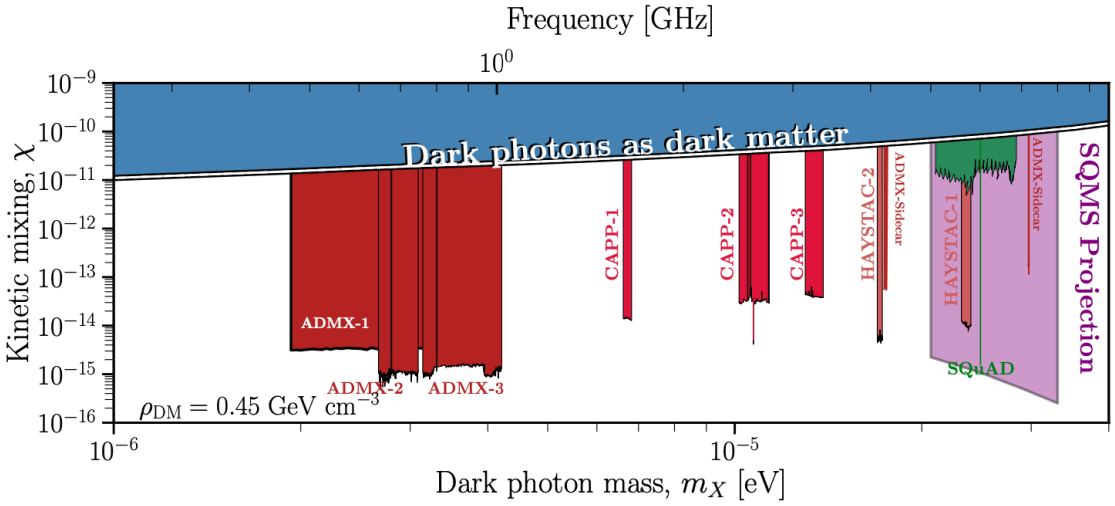

Figure 13: Projected sensitivity for dark photon searches.

4.2 Dixit et al.'s experiment with SQMS cavity

Dark though it is, the dark photon can be detected because of its kinetic mixing with the ordinary, visible photon. Because a dimension four operator may be created by multiplying the field strengths of two Abelian gauge fields, this kinetic mixing is always conceivable. The two gauge bosons can interact with one other as they propagate since such an operator exists. The portal connecting the visible and invisible worlds is created by this dynamic mixing. This portal is what enables the experiments to find the dark photon.

Now, let's describe briefly the protocol of Dixit's experiment. The setup is a cavity-qubit system for the parity measurement of photons in a Fock state of the resonator. The idea is to prepare the cavity empty and make a number of measurement by the T_1^{coh}. If the *qubit-based photon counter* which is based on Quantum non-Demolition (QND) techniques, observe a photon (a change of parity), hence that photon could come from a dark portal. Of course, the analysis of possible sources of photon coming from external noise, is really relevant here. In order to realize a single photon counter, we need to utilize the interaction between a superconducting transmon qubit and the field in a cavity, as described by the Jaynes-Cummings Hamiltonian in the dispersive limit ($g \ll \Delta \equiv |\omega_c - \omega_q|$). The Hamiltonian can be recast to elucidate a key feature: a photon number dependent frequency shift (2χ) of the qubit transition,

$$H/\hbar \simeq \omega_c a^\dagger a + \frac{1}{2}(\omega_q + 2\chi a^\dagger a)\sigma_z \, . \tag{42}$$

They used an interferometric Ramsey measurement of the qubit frequency to infer the cavity state. Errors in the measurement occur due to qubit decay, dephasing, heating, cavity decay, and readout infidelity, introducing inefficiencies or worse, false positive detections. $a^\dagger a$ is the number of photons operator. Therefore, if one photon in the cavity occurs, hence there is a frequency shift of 2χ for the qubit. We are working in the limit of $\bar{n} \ll 1$ so that n equals only to 0 or 1. Let's consider to go to the ω_q-rotating frame. Now, we prepare through a $\pi/2$-pulse the state of the qubit in the balanced superposition $(|g\rangle + |e\rangle)/\sqrt{2}$. The state is stationary in this frame. If a photon appears in the cavity, i.e. $n = 1$, hence the qubit state starts to precede with the 2χ frequency[6]. After an amount of time like $t = \pi/2\chi$, we apply a $-\pi/2$-pulse and if a photon appeared hence the qubit will be in the $|g\rangle$, otherwise in the $|e\rangle$ state. In this work, they used a device composed of a high quality factor ($Q_s = 2.06 \times 10^7$) 3D cavity used to accumulate and store the signal

[6]Here $|2\chi| = 2\pi \times 1.13$ MHz.

induced by the dark matter (storage, $\omega_s = 2\pi \times 6.011$ GHz), a superconducting transmon qubit ($\omega_q = 2\pi \times 4.749$ GHz), and a 3D cavity strongly coupled to a transmission line ($Q_r = 1.5 \times 10^4$) used to quickly read out the state of qubit (readout, $\omega_r = 2\pi \times 8.052$ GHz). See Figure 14.

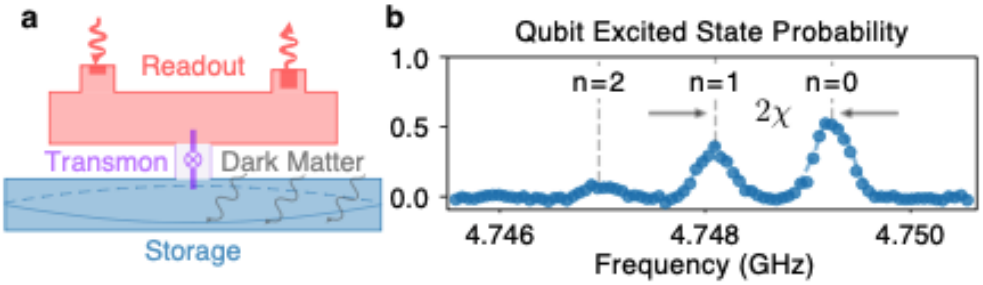

Figure 14: Setup Dixit's experiment.

In order to account for all possible error mechanisms during the measurement protocol, they modeled the evolution of the cavity, qubit, and readout as a *hidden Markov process* where the cavity and qubit states are hidden variables that emit as a readout signal. By counting photons with repeated parity measurements and applying a Markov model based analysis, they demonstrate single photon detection with background shot noise reduced to $-10\log_1 0\sqrt{\bar{n}_c} = 15.7 \pm 0.9$ dB below the quantum limit. They carried out a focused hidden photon search using this detection method. The injected $\bar{n}$ is far below the background population $\bar{n}_c$, and they collected $15,141$ separate observations where the interval between measurements is significantly greater than either the cavity or qubit timeframe. Dixit's group counted 9 photons in $15,141$ measurements. According for the systematic uncertainties of the experiment, a hidden dark photon candidate on resonance with the storage cavity ($m_{A'}c^2 = \hbar\omega_s$), with mixing angle $\epsilon > 1.68 \times 10^{-15}$ i sexcluded at the 90% confidence level. If we assume that $\rho_{DM} \simeq 0.4$ GeV$/c$m^3, hence Figure 15 shows the regions of hidden photon parameter space are excluded by the qubit based search.

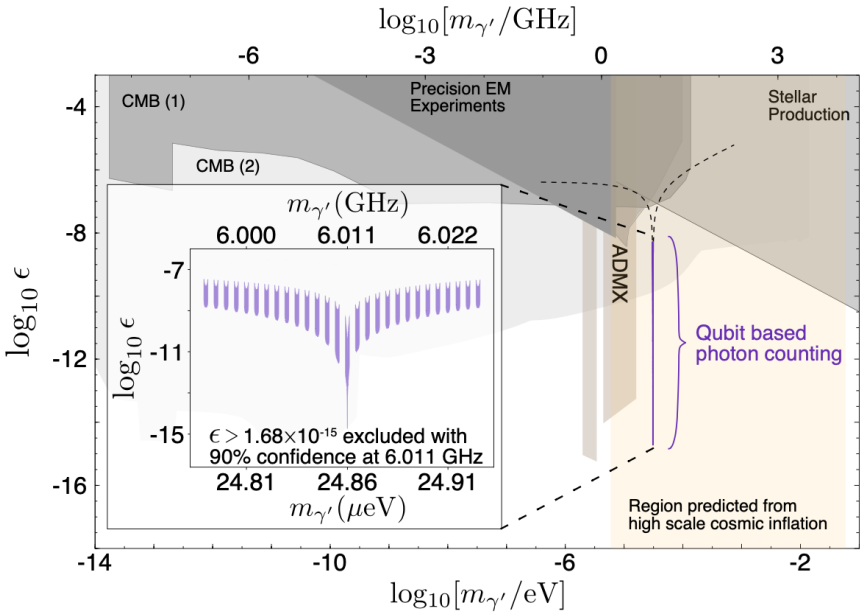

Figure 15: Hidden photon dark matter parameter space.

In the Ref. [6], the reader can find the set of parameters of the cavity-qubit system. We note

that the cavity's volume is $V = 11.3\ \mathrm{cm}^3$ and so

$$n_{df} \simeq \rho_{DM}/m_{df} \;\Rightarrow\; N_{df} \simeq n_{df} \cdot V \simeq \left(\frac{0.4\ GeV}{cm^3}\right) \times \left(\frac{1}{\mu eV}\right) \times 11.8\ cm^3 \simeq 10^{15}\ . \tag{43}$$

Extension to multiphoton Fock state? The real question is: *Can is there an advantage using a Fock state of the cavity with a huge number of photons*? The idea is to prepare the cavity in such state and waiting an amount of time as the coherence time T_1^{coh}. We expect that population of photons contained in the Fock state, will decrease exponentially. If we observe some peaks hence they could be photons coming from dark photons in the cavity there are 10^{15} of these. In Figure 16 is reported figuratively the viewing detection of dark photons.

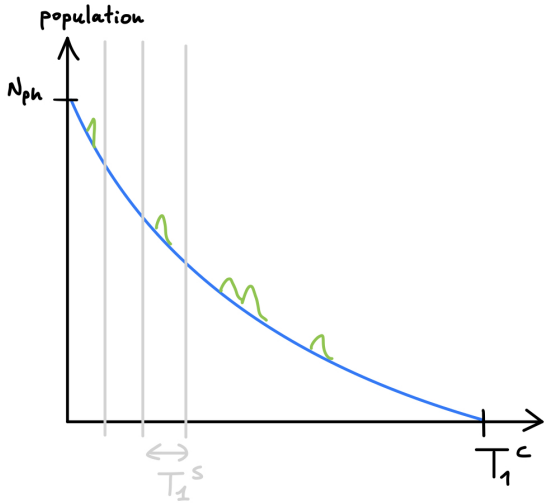

Figure 16: Possible trend of multiphoton detection of dark photons.

The point now is to understand if there are some benefits with this protocol. If we write down the Bolzmann equation associated to the rate decay of photons, w e find

$$\begin{aligned} \frac{df_\gamma}{dt} &= \Gamma_{\gamma' \to \gamma}(1 + f_\gamma) - \Gamma_{\gamma \to \gamma'}(1 + f_{\gamma'}) \\ &\propto f_{\gamma'}(1 + f_\gamma) - f_\gamma(1 + f_{\gamma'}) \\ &= f_{\gamma'} - f_\gamma \simeq f_{\gamma'} \end{aligned} \tag{44}$$

where in the last step we used that $N_\gamma \gg N_{\gamma'}$. Therefore, there are not advantages instead to perform single parity measurements. This fact brings us back on the Dixit's road. We could use the Dixit's protocol to reproduce the experiment at SQMS laboratory using cavities with a more performing Q and of different size. In this way, we could be able to explore a larger regime of possible masses for the dark matter candidate. For instance, the biggest SQMS cavity has a volume of $209.367\ cm^3$ and so a resonant frequency of ~ 3 GHz. With the same calculation we made in (43), we find that $N_{df} \simeq 10^{17}$. Therefore, increasing the volume of the cavity we are changing the mass regime and there will be more[7] dark photons inside the cavity. We might expect that the photon rate increases.

[7]Always if we assume that $\rho_{DM} \simeq 0.4\ \mathrm{GeV}/\mathrm{cm}^3$.

5 Conclusion

In this report we did a kind of review about the progress that the SQMS group achieved in the last few years about the SRF cavities for GW detection. We saw in Figure 8 that the supremacy for the projected sensitivity in the GW detection, is detained by the theoretical work of Berlin et al. in Fermilab. We analyzed briefly the possibility to consider also a qubit inside the cavity in order to understand if it could have an advantage in the sensitivity. The hope is that is does but a deeper study is necessary. A hard theoretical work which is fundamental to study is the direct qubit-GW interaction. To understand this interaction would mean to unify the linearized GR with quantum formalism of qubit. In the second part of this report we reviewed the Dixit's experiment for searching dark photons with superconducting qubit trying to understand if there are some advantages to use multiphoton Fock modes. The answer we gave ourselves is *no*. A possible project for the Master Thesis of the author is to reproduce at Fermilab, the Dixit's setup of the experiment and use different cavities more performing in terms of Q and V_{cav}. In this way we could have a greater sensitivity, we could exclude or detect (we hope) dark photon for different regime of mass $m_{df} = \hbar\omega_s/c^2 \propto 1/L_{cav}$.

References

[1] V. B. Braginskii, M. B. Menskii, *High-Frequency Detection for Gravitational Waves*, Jetp Letters, Vol. 3, No. 11 (1971).

[2] F. Pegoraro, E. Picasso, L. A. Radicati, *Electromagnetic Detector for Gravitational Waves*, J. Phys., Vol. 11, No. 10 (1978).

[3] A. Berlin et al., *Searches for new particles, dark matter, and gravitational waves with srf cavities*, arXiv preprint arXiv:2203.12714 (2022).

[4] A. Berlin et al., *Detecting High-Frequency Gravitational Waves with Microwave Cavities*, arXiv preprint arXiv:2112.11465v1 (2021).

[5] R. Ballantini, Ph. Bernard, E. Picasso et. al, *Microwave Apparatus for Gravitational Waves Observation*, arXiv:gr-qc/0502054v1 (2005).

[6] A. V. Dixit et al., *Searching for Dark Matter with Superconducting Qubit*, PRL, 126 (2021).

[7] M. Maggiore, *Gravitational Waves. Vol. 1: Theory and Experiments*, Oxford Master Series in Physics (Oxford University Press, 2007).

[8] C. W. Misner, K. S. Thorne, J. A. Wheeler, *Gravitation*, Macmillan (1973).

[9] M. Fabbrichesi, E. Gabrielli, G. Lanfranchi, *The Dark Photon*, arXiv:2005.01515v3 (2021).

[10] A. Berlin, R. T. D'Agnolo et al., *Axion Dark Matter Detection by Superconducting Resonant Frequency Conversion*, arXiv:1912.11048v1 (2019).

[11] Nancy Aggarwal et al., *Challenges and opportunities of gravitational-wave searches at MHz to GHz frequencies*, arXiv:2011.12414 (2021).

[12] R. T. D'Agnolo, *Waves in a box: SRF cavities for GW detection*, UHF-GWs Talk (2021).

A TT-frame and proper detector frame

Let's parameterize the trajectory of a particle in a curved space-time $g_{\mu\nu}$ with the proper time τ : $x^\mu(\tau)$. The *geodetic equation*,

$$\frac{d^2x^\mu}{d\tau^2} + \Gamma^\mu_{\nu\rho}(x)\frac{dx^\nu}{d\tau}\frac{dx^\rho}{d\tau} = 0\ , \tag{45}$$

describes the equation of motion for this particle in the curved background, in absence of external non-gravitational forces. If we consider two nearby geodesics $\{x^\mu(\tau), x^\mu(\tau)+\xi^\mu(\tau)\}$ and we take the difference between them, we find the equation of geodetic deviation,

$$\frac{D^2\xi^\mu}{D\tau^2} = -R^\mu{}_{\nu\rho\sigma}\xi^\rho u^\nu u^\sigma \tag{46}$$

which shows that a tidal gravitational force, determined by the Riemann tensor, is experienced by two time-like geodesics.

A.1 The TT-frame

There exist a gauge where GWs have an especially simple form, the TT gauge. We denote the corresponding reference frame as the TT frame and we ask what it means, physically, to be in the TT-frame. From the geodetic equation (45) we see that if a test mass is at rest at $\tau = 0$ (so that $dx^i/d\tau = 0$) then

$$\begin{aligned} \frac{d^2x^i}{d\tau^2}\Big|_{\tau=0} &= -\Big[\Gamma^i_{\nu\rho}(x)\frac{dx^\nu}{d\tau}\frac{dx^\rho}{d\tau}\Big]_{\tau=0} \\ &= -\Big[\Gamma^i_{00}\Big(\frac{dx^0}{d\tau}\Big)^2\Big]_{\tau=0} . \end{aligned} \tag{47}$$

Writing $g_{\mu\nu} = \eta_{\mu\nu} + h_{\mu\nu}$ and expanding to first order in $h_{\mu\nu}$ we find a simple form for Christoffel symbol so that

$$\Gamma^i_{00} = \frac{1}{2}(2\partial_0 h_{0i} - \partial_i h_{00}) . \tag{48}$$

In the TT gauge this quantity vanishes, because both h_{00} and h_{0i} are set to zero by the gauge condition. Therefore, if at time $\tau = 0$ we have $dx^i/d\tau = 0$ hence $d^2x^i/d\tau^2 = 0$. So $dx^i/d\tau$ remains zero at all times. That shows that a particle which was at rest before the arrival of the GW, remains at rest even after the GW passed. A physical implementation of TT gauge can be obtained using the free test masses themselves to mark the coordinates.

A.2 The proper detector frame

The TT frame has the advantage that GWs have a very simple form in it. However, it is not the frame normally used by an experimentalist to describe its apparatus. In a laboratory, positions are not marked by freely falling particles; rather, after choosing an origin, one ideally uses a rigid ruler to define the coordinates. Conceptually, the simplest laboratory to analyze is one in free fall in the total gravitational field. If we restrict our attention to a sufficiently small region of space we can choose coordinates so that even in presence of GWs, the maetric is flat. We can construct such a freely falling frame along an entire geodetic using the FNC. The corrections to flat space present only from the second order of derivatives. We can see that if x is the typical variation scale of the metric, so that $R_{\mu\nu\rho\sigma} = \mathcal{O}(1/x^2)$ hence the corrections to the flat metric are $\mathcal{O}(r^2/x^2)$, where $r = x^i x_i$. If we want to find the metric for Earthbound detector we can explicitly write the coordinate transformation form the inertial frame to the frame which is accelerating and rotating, and transform the metric accordingly. We find, up to second order in r, that

$$\begin{aligned} ds^2 \simeq & -dt^2(1 + \overbrace{2\mathbf{a}\cdot\mathbf{x}}^{\text{inert. acc.}} + \overbrace{(\mathbf{a}\cdot\mathrm{x})^2}^{\text{grav. redshift}} - \overbrace{(\mathbf{\Omega}\times\mathbf{x})^2}^{\text{rotation t-dilate}}) \\ & + 2dtdx^i\Big(\overbrace{\epsilon_{ijk}\Omega^j x^k}^{\text{Sagnac effect}} - \frac{2}{3}R_{0jik}x^i x^k\Big) + dx^i dx^j\Big(\delta_{ij} - \frac{1}{3}R_{ikjl}x^k x^l\Big) . \end{aligned} \tag{49}$$

B GW sources

Possible sources of GWs in the frequency range of MHz $\div$ GHz are binary merges of ultralight compact objects with mass $M \lesssim 10^{-11} M_\odot$ and GWs emitted by the superradiant axion cloud around spinning primordial black holes, corresponding to masses of $M \sim 10^{-4} M_\odot$. We report below two pictures as examples of coherent and stochastic sources of GWs.

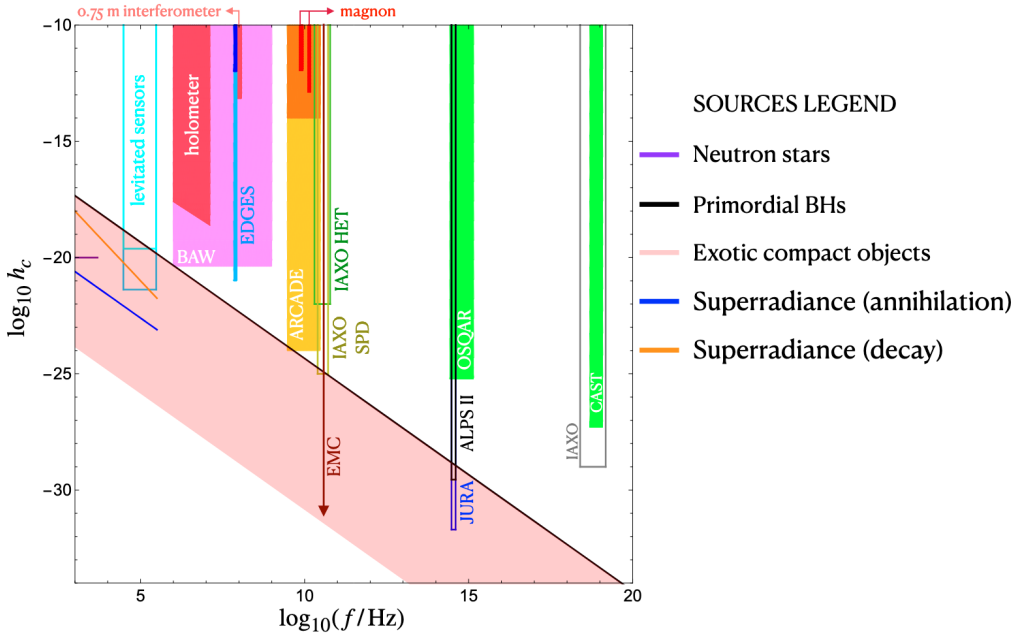

(a) Coherent sources.

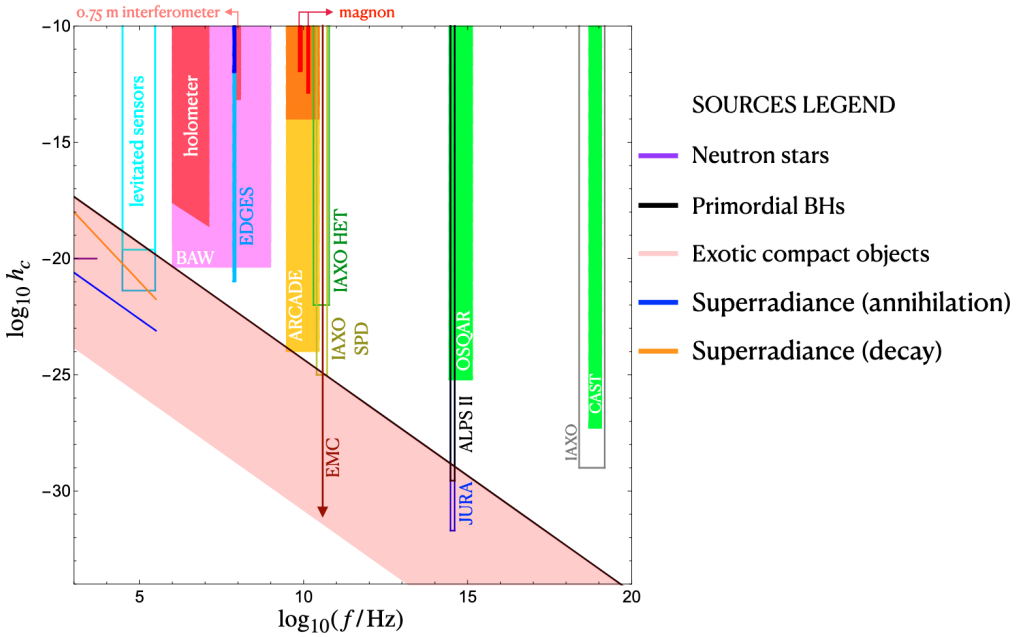

(b) Stochastic sources.